High Perform. Polym. **12** (2000) 621–629. Printed in the UK PII: S0954-0083(00)19128-7

Anomalies in the optical index of refraction of spun cast polystyrene thin films

Xuesong Hu†, Kwanwoo Shin†, Miriam Rafailovich†, Jonathan Sokolov†, Richard Stein‡, Yee Chan§, Kurt Williams‖, W L Wu¶ and Rainer Kolb+

† Department of Materials Science and Engineering, State University of New York at Stony Brook, Stony Brook, NY 11794, USA
‡ Department of Chemistry and Engineering, University of Massachusetts at Amherst, Amherst, MA 01003, USA
§ Wheatley High School, Old Westbury, NY 11568, USA
‖ Veeco Instruments Inc, Plainview, NY 11803, USA
¶ National Institute of Standards and Technology, Gaithersburg, MD 20899, USA
+ ExxonMobile Research and Engineering Company, Annandale, NJ 08801, USA

Received 17 November 2000

Abstract. We used x-ray reflectivity in combination with optical ellipsometry to measure the optical index of refraction, n, in thin spun cast polystyrene films. We have found that n is independent of the molecular weight, but is a sharp function of the film thickness for films less than 100 nm. In all cases the deviation from the bulk, Δn, is negative and varies linearly with wavelength in the visible region. The magnitude of Δn, was found to be as large as 0.25 for films 7 nm thick. The bulk index of refraction was recovered in all films after annealing for 2 h above T_g at 160 °C. X-ray reflectivity measurements of the scattering critical angle show minimal density deviations from the bulk (less than 0.5%) between the annealed and unannealed films. Consequently the large molecular-weight-independent value of Δn is interpreted as being due to a radially symmetric segmental orientation induced by the spinning process.

1. Introduction

Thin-film coatings are commonly used to optically match the refractive index of lenses and minimize reflections in optical components. In order for these coatings to be effective it is important to determine their optical constants with high accuracy. It is well established that stress can affect the optical properties of polymer films. Previous studies [1], in particular those by Prest [2, 3] and coworkers [4–6], have shown that spinning and solvent casting processes can induce stress in polymer films, which is detected by a change in the optical birefringence. The thickness, t, of the films in these studies ranged from $0.5\ \mu m < t < 10\ \mu m$. These values are comparable to optical wavelengths and hence changes in the optical birefringence could easily be detected. In this paper we concentrate on the effects of spin casting on very thin films.

When the film thickness becomes less than the wavelength of the analysing light, it becomes difficult to obtain simultaneous measurements of the thickness and the refractive index with single-wavelength ellipsometry. Therefore, to calculate the optical refractive index of very thin films, we show that it is possible to use simultaneous x-ray reflectivity and optical ellipsometry. X-ray reflectivity can be used to measure the exact thickness of polystyrene thin

0954-0083/00/040621+09$30.00 © 2000 IOP Publishing Ltd

films and single-wavelength ellipsometry can then be used to calculate the optical refractive index [7].

2. Experimental details

2.1. Methods

Monodisperse polystyrene (PS) films of $Mw = 90\,000$ and $2\,650\,000$ (Polymer Laboratories, $Mw/Mn < 1.02$) were spun cast onto native oxide covered Si wafers from a toluene solution at 2500 rpm. The thickness of the films was controlled by varying the viscosity of the solution. The results for the two molecular weights were identical and hence the data are combined in the figures below.

Immediately after spin casting and prior to annealing, the thicknesses of the PS films were measured by x-ray reflectivity. Single-wavelength optical ellipsometry was then performed to calculate the optical refractive index. The thicknesses of the films were kept fixed at the values obtained in the reflectivity measurements and a one-parameter fit was performed to yield only the optical index of refraction. The samples were then annealed at 125 °C ($T_g = 103$ °C) under a vacuum of 10^{-3} Torr for 2 h. The x-ray reflectivity thickness measurements and the calculation of the optical refractive index were then performed again. This procedure was checked independently on one sample, a 129 Å thick PS film which was also analysed by multiple-wavelength ellipsometry at Veeco instruments.

2.2. Ellipsometer: AutoEL-II

The AutoEL is a microprocessor-controlled automatic-nulling ellipsometer that measures changes in the state of polarization of a laser beam reflected from sample surfaces by determining the azimuth P of a rotatable polarizer prism in the incident beam and the azimuth A of a rotatable analyser prism in the reflected beam and for which the intensity of the reflected beam (after passage through the analyser) is a minimum. From the measured azimuths P and A at 'extinction', the instrument computes two intermediate parameters Δ and Ψ which can be used to calculate the optical constants of bare surfaces, and the thickness and refractive index on those surfaces. The intermediate parameters Δ and Ψ are alphanumerically displayed and are also transmitted in ASCII RS232 serial format for use by digital computers or other external equipment. The polarizer azimuth P at null is a measure of Δ, and the analyser azimuth A at null is a measure of Ψ. For the PCSA (polarizer, compensator, sample, analyser; which describes the sequence in which the light from the source passes through the instrument) nulling configuration, equations relating P and A at null to Δ and Ψ are simple linear equations in the form

$$\rho = \tan \Psi e^{i\Delta}. \tag{1}$$

2.3. X-ray reflectivity

The measurements were performed at Beamline X10B at the National Synchrotron Light Source (NSLS) at Brookhaven National Laboratory (Upton, USA) using an incident beam energy of 11 keV which corresponds to a wavelength of $\lambda = 1.1271$ Å. The scattering geometry for specular reflectivity is shown in figure 1.

The wavevector transfer $\vec{q} = \vec{k}_f - \vec{k}_i$ where $\vec{k}_r$ and $\vec{k}_i$ are the incident and scattered wavevectors, respectively, which are controlled by varying the incident (α_i) and exit (α_f) angle

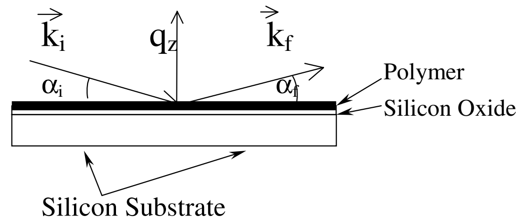

Figure 1. Scattering geometry used for x-ray reflectivity measurements.

and are defined as

$$q_z = 2\pi/\lambda(\sin\alpha_i + \sin\alpha_f) \qquad q_x = -2\pi/\lambda(\cos\alpha_i - \cos\alpha_f). \tag{2}$$

The specular reflectivity is taken at $q_x = 0$ as a function of q_z by varying the α_i and α_f while maintaining $\alpha_i = \alpha_f$. Since the specular reflectivity detects the variation of the electron density $\rho(z)$ in the direction normal to the surface, averaged in the (x, y)-plane, it is sensitive to the layer thicknesses, the density contrasts and the interfacial roughnesses defined by the probability density.

To analyse the reflectivity data the recursive Parratt formalism has been used [8] where we assume a two-layer model; an infinitely thick Si substrate covered by a thin Si oxide layer and a thin PS layer. The roughnesses of the PS film, σ_1 and σ_2, at the air and Si oxide interfaces, respectively, were taken into account by modified Fresnel reflection coefficients. The scattering intensity $I(q_z)$ of the reflectivity as a function of the film thickness d and the roughnesses is best expressed within the Born approximation [9] given by

$$I(q_z) \propto \frac{1}{q_z^4}\left|\int \frac{\mathrm{d}\rho(z)}{\mathrm{d}z}\exp(-\mathrm{i}q_z z)\right|^2. \tag{3}$$

Qualitatively, equation (3) contains damping factors due to the surface roughnesses and an oscillating term (with so-called Kiessig fringes) due to the interference of the scattering between both surfaces. The oscillation period, $\Delta q_{z,0}$, is related to the film thickness, d, and can be used to approximate the thickness,

$$d = 2\pi/\Delta q_{z,0}. \tag{4}$$

The z-direction is taken normal to the sample surface while the projection of the incident wavevector k_i on the surface is used to define the y-direction. Specular scans are intensity against angle (or q_z) spectra, where θ is varied and $q_z = (4\pi/\lambda)\sin\theta$. The specular reflectivity thus measured is mostly sensitive to variations in electronic density in the direction normal to the surface.

3. Results

3.1. X-ray reflectivity

Figure 2 shows the reflectivity spectra obtained from unannealed samples of PS of $Mw = 2\,650\,000$ of four different thicknesses in the range 127–500 Å. From the figure one can see the period of the Kiessig fringes gradually decreases as the thickness of the films increases. The full curves are fits to the model, i.e. a single PS layer on a native oxide covered substrate, 10–20 Å thick and with an interfacial roughness of $\sigma_1 \sim 10$ Å and $\sigma_2 \sim 2$ Å.

The samples were then examined by ellipsometry and annealed for 2 h at 125 °C. The data are shown in figure 3 and the full curves correspond to fits with a similar model. The fitting

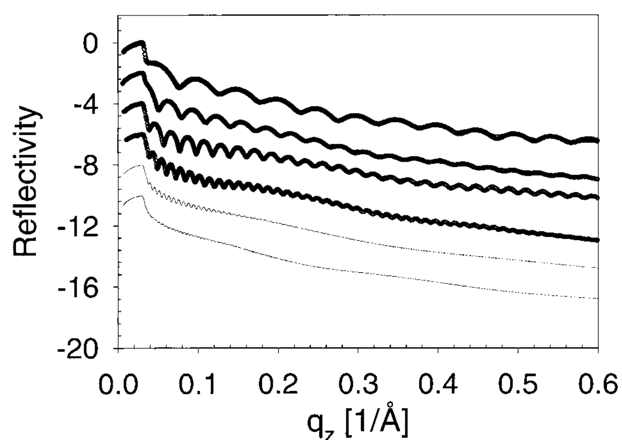

Figure 2. X-ray reflectivity spectra as a function of film thickness for PS ($Mw = 2\,650\,000$) prior to annealing.

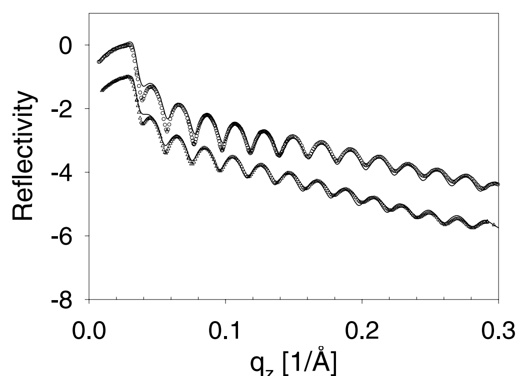

Figure 3. Fitting results of a PS thin film (300 Å) before and after annealing.

values for all the samples are tabulated in table 1. Comparing the results of the as-cast and the annealed films we find that the film thickness decreases slightly (less than 12 Å) in all cases upon annealing. The roughness at the free surface and the silicon oxide interface does not change much. The oxide layer thickness also remains unchanged in the annealing process.

The results for the change in the film thickness with annealing are summarized in figure 4 where we see that for all thicknesses larger than 1000 Å, the thickness of the films decreases by approximately 10 Å following annealing.

X-ray reflectivity can be a good method to measure the absolute density of a thin film. The critical angle for a reflection at an interface can be derived form the Snell–Descarte law, where we assume that the refractive index of vacuum is $n = 1$,

$$n_1 \cos\theta_1 = n_2 \cos\theta_2 \tag{5}$$

where n is the index of refraction for the x-rays, which is one in vacuum and in a medium is given by;

$$n = 1 - \delta - \mathrm{i}\beta \tag{6}$$

where δ and β are the scattering and absorption cross sections given by

$$\delta = \lambda^2 \rho_{\mathrm{el}} r_0 / 2\pi \qquad \text{and} \qquad \beta = \mu\lambda/4\pi \tag{7}$$

Table 1. The fitting values for all of the samples.

	PS			SiO_2	
	t	δ[a]	$\sigma_{\text{air-PS}}$	t	$\sigma_{\text{PS-SiO}}$
Before annealing					
Ps2	126.9	1.774	6.30	20.1	2.67
Ps3	206.0	1.752	9.06	19.8	1.67
Ps4	298.0	1.730	6.31	14.2	1.83
Ps5	507.1	1.889	9.64	15.1	3.29
Ps6	973.8	1.85	10.1	16.7	3.22
Ps7	1325.2	1.750	8.1	19.8	3.06
After annealing					
Ps2	129.2	1.731	7.3	18.9	1.77
Ps3	199.2	1.836	5.6	20.2	2.97
Ps4	302.6	1.767	8.44	21.8	2.00
Ps5	505.9	1.873	9.64	23.1	2.34
Ps6	964.1	1.830	11.1	22.0	2.20
Ps7	1314.9	1.728	9.42	20.8	2.56

[a] The dispersion coefficient δ is the real factor of refractive index $n = (1 - \delta)$ and can be written by $\delta = \lambda^2 \rho_{\text{el}} r_0 / 2\pi$, where λ, ρ_{el} and r_0, are the wavelength of x-ray (1.1273 Å), the electron density of materials and the electron radius (2.82×10^{-13} cm) respectively.

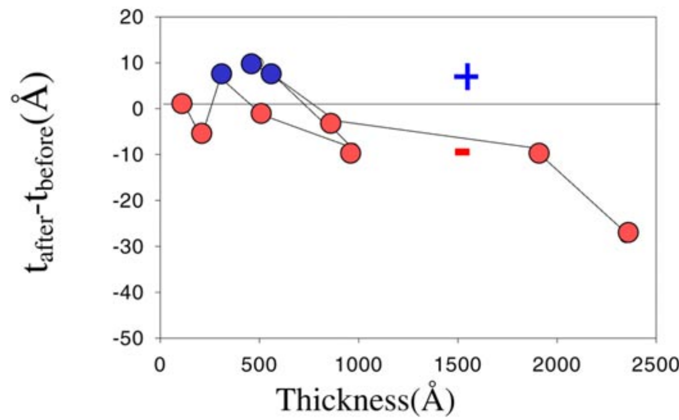

Figure 4. Thickness difference between the annealed and unannealed samples.

where ρ_{el} is the electron density and r_0 is the classical electron radius, $r_0 = 2.8 \times 10^{-10}$ nm. For incident angles smaller than a minimum value, θ_c, the total external reflection of the radiation will occur. Combining equations (5)–(7) we can derive the relationship between for the critical wavevector, q_c, and the electron density,

$$q_c = 4\pi/\lambda(\sin(\theta_c)) \qquad \text{where } \theta_c \sim (2\delta)^{1/2} \text{ and } \beta \sim 0. \tag{8}$$

The values for θ_c and q_c at $\lambda = 1.1271$ Å for SiO, Si, and PS are tabulated in table 2.

Figure 5 shows the reflectivity spectra expanded to show the intensity at low values of q, from a sample 533 Å thick before and after annealing. From the figure we can see that the reflected intensity is essentially one for $q < q_c^{\text{Si}} = 0.0317$, where q_c^{Si} is the critical wavevector for the silicon oxide substrate. We can also see that frequency for the first oscillation for $q > q_c^{\text{Si}}$ of the reflected intensity is somewhat higher after annealing, indicating that the film has become slightly thicker. A slight dip in the intensity is observed at $q = 0.022$, which corresponds to the

Table 2. Parameters for x-ray reflectivity from PS films coated on silicon wafers.

	δ	θ_c	q_c (Å^{-1})
Si	4.0377×10^{-6}	2.84×10^{-3}	0.0317
SiO	4.0286×10^{-6}	2.84×10^{-3}	0.0317
PS	1.9955×10^{-6}	2.00×10^{-3}	0.0222

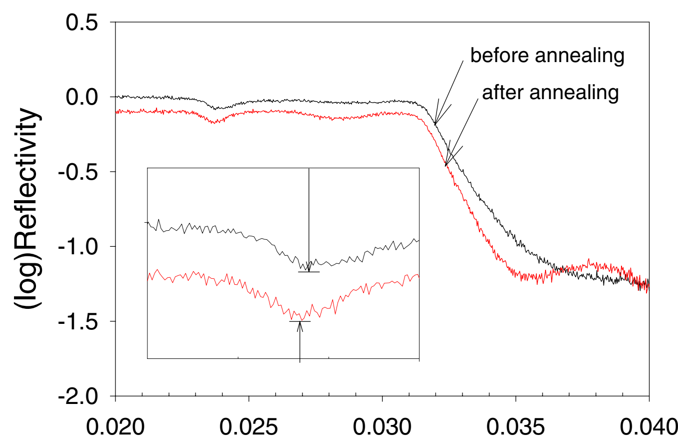

Figure 5. X-ray reflectivity near the critical angle for a PS film 970 Å thick.

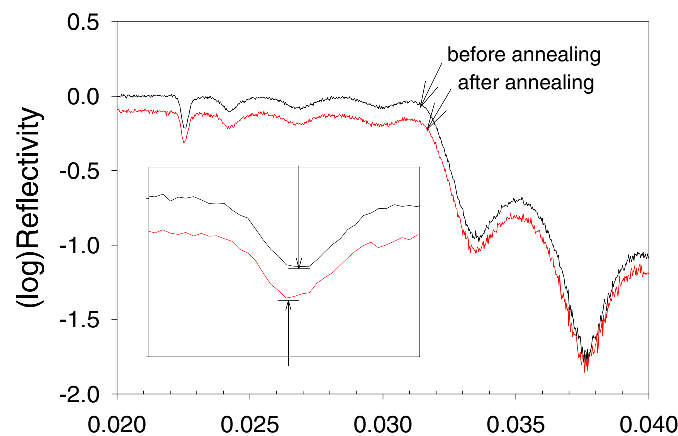

Figure 6. Expanded section of x-ray reflectivity spectra performed on a rotating anode source showing the shift in the critical angle for the PS–air interface before and after annealing the PS films at $T = 125\,^{\circ}\mathrm{C}$ using 1150 Å thick films The inset shows the scattered intensity around the dip at $q = 0.022$.

critical wavevector of PS, $q_c^{PS} = 0.0222$. This dip is far smaller than that observed at q_c^{Si} since most of the scattered intensity originates from the Si interface. The scattered intensity around this dip is plotted in the inset. From the figure we can see a slight shift of 0.3%, indicating that the electron density of the films is slightly higher prior to annealing. Figure 6 shows the reflectivity at low q for a 1150 Å thick PS film. It is interesting to note that, as expected, no oscillations are visible for $q < q_c^{PS}$ and a low-amplitude oscillation becomes visible for $q > q_c^{PS}$. In this

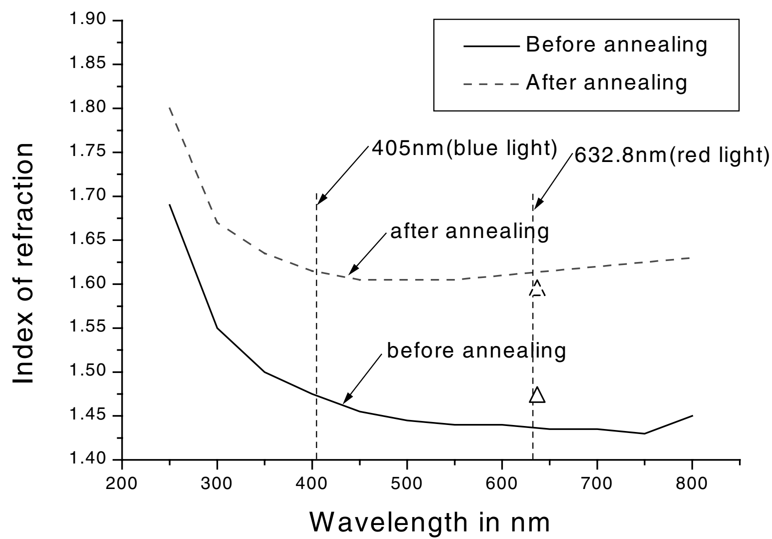

(a)

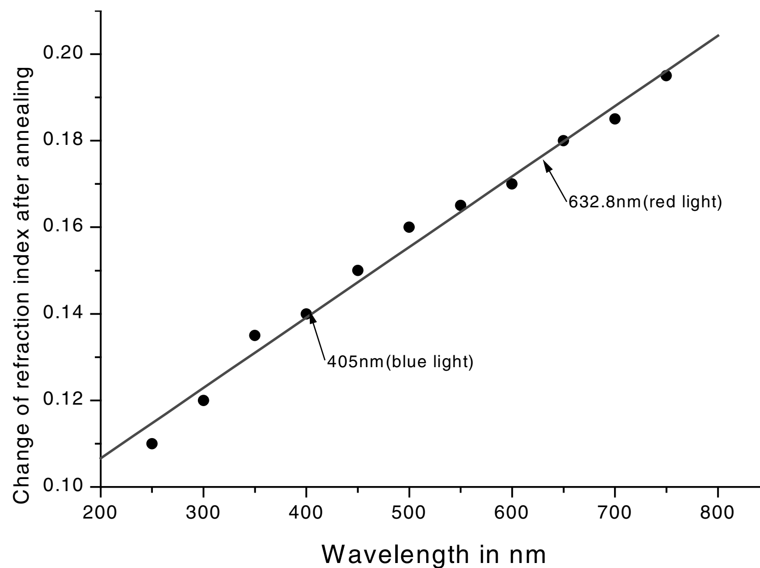

(b)

Figure 7. (a) Index of refraction as measured by variable-wavelength ellipsometry, as a function of wavelength for PS films 12.9 nm thick. (b) Deviation of the index of refraction between annealed and unannealed samples as a function of the wavelength. The solid line is a straight line to fit the data.

case, also, the electron density is slightly higher prior to annealing, with a change of 0.3%. This data is inconsistent with the previously held assumption that spun cast films are thicker because they are ‘fluffy’, i.e. they contain voids left behind by the rapidly evaporating solvent. Since the PS films become glassy immediately after the solvent is removed, the films need to be annealed to collapse back to their bulk density. The density difference we observe is of the wrong sign and too small in magnitude to explain the difference in the thickness.

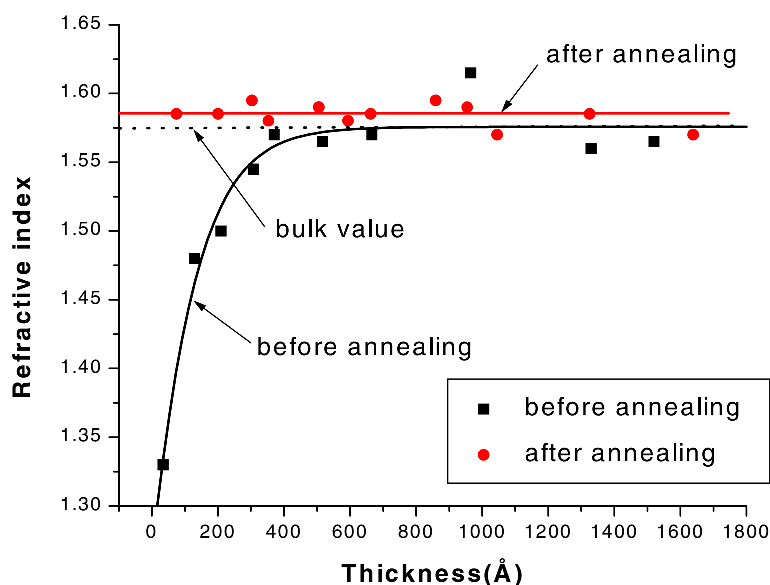

Figure 8. Index of refraction as a function of PS film thickness.

3.2. Ellipsometry

The most significant difference between the unannealed and annealed films is the change in the optical index of refraction upon annealing. In figure 7(a) we plot the index of refraction, n, as a function of the wavelength for a 129 Å thick film, before and after annealing, and in figure 7(b) we plot the change in the index Δn after annealing as a function of wavelength. From the latter figure we can see that Δn increases almost linearly with wavelength with an average value of $\Delta n = 0.16$ for an optical wavelength of around 500 nm.

In order to obtain an accurate measure of the index of refraction with a single-wavelength ellipsometer we used the thickness values from table 1 as input parameters and performed a fit with n as the only free parameter. The results from this method for a film of thickness 129 Å are superimposed as a triangle in figure 7(a) where we see that the measurement from the variable and single-wavelength ellipsometry yield comparable results.

In figure 8 we plot n as a function of the film thickness, t, before and after annealing, as obtained from single-wavelength ellipsometry at $\lambda = 6328$ Å. From the figure we can see that in the unannealed film n decreases rapidly with the film thickness for $t < 60$ nm. After annealing for 2 h at 125 °C the bulk value of n is restored. Since we see almost no change in the x-ray reflectivity critical angles for PS, the large decrease in the index of refraction as a function of the film thickness observed in the unannealed films cannot be explained by a change in density. Large shifts in the index of refraction are known to occur when polymer chains are mechanically rubbed [10, 11]. These shifts, which are also negative, are attributed to the segmental orientation of specific groups on the polymer chains which induce an optical retardation in a specific direction relative to the rubbing direction. Orientation produced in the spin casting process is usually radially symmetric about the spin axis and uniformly either in or out of the plane of the spun cast film. Hence we can define an effective optical retardation which is equivalent to the difference between the bulk value of n and the measured value of n in the spun cast films, i.e. Δn which is plotted in figure 7(b). From the figure we can

see that the average values of $\Delta n > 0.1$ are at least an order of magnitude larger than those previously reported in the rubbed films of comparable thickness. Hence highly oriented films are produced by the spinning process. Further work is in progress where we will study the time and temperature dependence of Δn in order to learn more regarding the effect of surface interactions on segmental orientation.

4. Conclusions

By using x-ray reflectivity in combination with optical ellipsometry we have found that the optical index of refraction in spun cast films is independent of the molecular weight but a sharp function of the film thickness for films less than 100 nm thick. For a given thickness the deviation from the bulk value is negative and varies linearly with wavelength in the visible region. The magnitude of the deviation, Δn, was found to be as large as 0.25 for 7 nm thick films. The bulk index of refraction was recovered in all films after annealing for 2 h above T_g at 160 °C. X-ray reflectivity measurements of the scattering critical angle show minimal density deviations from the bulk (less than 0.5%) between the annealed and unannealed films. Consequently, the large molecular-weight-independent value of Δn observed is interpreted as being due to radially symmetric segmental orientation induced by the spinning process.

References

[1] Groll S G 1979 *J. Appl. Polym. Sci.* **23** 847
[2] Prest W M 1979 *J. Appl. Phys.* **50** 6067
[3] Prest W M 1980 *J. Appl. Phys.* **51** 5170
[4] Beaucage G J 1993 *J. Polym. Sci.* B **31** 319
[5] Ree M 1993 *Polymer* **34** 1423
[6] Cammarata R C 1999 *Mater. Res. Soc. Bull.* **24** 34
[7] Russell T P 1990 *Mater. Sci. Rep.* **5** 171
[8] Parratt L G 1954 *Phys. Rev.* **95** 359
[9] Sinha S K, Sirota E B, Garoff S and Stanley H B 1988 *Phys. Rev.* B **38** 2297
[10] Hong S D, Chang C and Stein R S 1975 *J. Polym. Sci.* B **13** 1447
[11] Schwab D A, Agra D M G, Kim J, Kumar S and Dhinojwala A 2000 *Macromolecules* **33** 4903